Communication

A Wideband Circularly Polarized Tightly Coupled Array

Long Zhang, Steven Gao, Qi Luo, Wenting Li, Yejun He, and Qingxia Li

***Abstract*— Tightly coupled arrays (TCAs) have received considerable interests recently. Although various TCAs have been reported, they are generally limited to single or dual linear polarizations. Considering the importance of circularly polarization in various wireless systems, it is meaningful to design a circularly polarized (CP) TCA with a simple configuration. This communication presents a CP tightly coupled crossed dipole array (CP-TCCDA) with intrinsic CP feeding structure, which achieves wide overlapped impedance bandwidth and axial ratio (AR) bandwidth. An analysis is given to explain the principles of AR bandwidth improvement and is validated by the comparison of radiated E-fields between a CP-TCCDA and a conventional CP crossed dipole array. To verify the design concept, a 4 × 4 CP-TCCDA with elaborate feeding network is fabricated and measured. The measured results confirm that the proposed array achieves VSWR < 3 bandwidth from 2.06 to 6.46 GHz (3.14:1) and 3 dB AR bandwidth from 2.35 to 5.6 GHz (2.38:1), which are much wider than the bandwidth of an isolated element and a conventional array using the same element.**

***Index Terms*— Circular polarization (CP), crossed dipole, tightly coupled array (TCA), wideband array.**

I. Introduction

With the rapid development of various wireless communication systems, wideband antennas and arrays are becoming increasingly important to multifunctional systems, high-data-rate communication links, high-resolution radar and tracking systems, software radios, and electronic warfare applications [1]. To design wideband arrays, wideband antenna elements, such as the Vivaldi antenna and "bunny-ear" antenna are normally used. However, the considerable height limits their applications to some extent.

Instead of using elements with inherent broad bandwidth to build a wideband array, Munk [2] used capacitively coupled short dipoles to design a wideband array which achieved 4.5:1 impedance bandwidth. The idea was to alleviate inductive loading introduced by the ground plane using capacitive coupling among neighboring elements. Due to the closely spaced dipole configuration, these elements are tightly coupled and the electric current along each dipole is almost constant, which is distinct from the electric current on a single dipole where a sinusoidal magnitude distribution with nulls at the termination exists [3]. This kind of dipole array emulated Wheeler's electric current sheet which can support radiation at much lower frequencies than the element's self-resonant frequency [4].

Two different types of arrays were proposed to realize Wheeler's current sheet and both obtained wide bandwidth. The first one was the "connected array" which interconnected array elements to achieve relatively constant electric current across the array aperture and large array bandwidth [5], [6]. Another type was the "tightly coupled array" (TCA) which utilized closely spaced dipoles, where the strong mutual coupling among the dipole elements facilitated the improvement of array bandwidth [7], [8].

Although the aforementioned arrays achieved several octave bandwidths, they were all linearly polarized or dual linearly polarized and only the improvement of impedance bandwidth was considered. For applications such as the high-data-rate satellite communications, wideband circularly polarized (CP) antennas and arrays are preferred [9]. However, there are few reported CP array designs based on the concept of connected array or TCA. A dual-CP spiral array in which neighboring spirals of orthogonal polarizations were connected and achieved 1.8 times axial ratio (AR) bandwidth than the single spiral [10]. The AR bandwidth enhancement in this design was mainly due to the doubling of the traveling-wave electric current path. By connecting more spirals in a ring-array structure, the AR bandwidth was further improved [11]. A spiral array within which the arms of the spiral elements were interwoven achieved a 10:1 bandwidth [12]. However, within this 10:1 frequency range, the average difference between the RHCP and LHCP gains were only 7 dB indicating that the AR performance of the array was not good.

Recently, a crossed dipole structure which incorporated 90° phase-shift line between the orthogonally placed dipoles was presented [13]. Because of the incorporated 90° phase-shift line, the crossed dipole antenna was able to be fed by a coaxial connector directly without any baluns and still achieved good CP performance. Based on the CP crossed dipole, a CP TCA with intrinsic CP feeding structure is developed in this communication. The proposed design utilizes two orthogonally polarized E-fields but is different from the dual-polarized TCA [14] where the dipoles of different polarizations were fed offset by $\lambda/4$. In the proposed design, the orthogonally polarized dipoles are fed concentrically with inherent 90° phase shift, which eliminates the need of external 90° hybrids for a dual-polarized TCA to produce CP radiation. By decreasing the element space and choosing appropriate overlapped structure between adjacent elements, it is shown that not only the impedance bandwidth but also the AR bandwidth of the array is greatly improved compared with the single isolated element. To verify the concept, a 4 × 4 array is prototyped, and the measurement results confirm that the proposed CP TCA achieves a 3.14:1 VSWR < 3 bandwidth and a 2.38:1 3 dB AR bandwidth, which shows much wider bandwidth than the conventional crossed dipole array using the same element.

II. Tightly Coupled Crossed Dipole Unit Cell

A. Unit Cell Configuration

To predict the performance of an infinite array, the unit cell under periodic boundary gives a good approximation. The configuration of the tightly coupled crossed dipole unit cell is shown in Fig. 1.

Manuscript received February 23, 2017; revised May 16, 2018; accepted July 22, 2018. Date of publication August 24, 2018; date of current version October 29, 2018. This work was supported in part by the National Natural Science Foundation of China under Grant 61801299 and Grant 61372077, in part by the Guangzhou Science and Technology Program under Grant 201707010490, and in part by the Shenzhen Science and Technology Programs under Grant JCYJ20170302150411789, Grant JCYJ20170302142515949 and Grant GCZX2017040715180580. *(Corresponding author: Yejun He.)*

L. Zhang and Y. He are with the Shenzhen Key Laboratory of Antennas and Propagation, College of Information Engineering, Shenzhen University, Shenzhen 518060, China (e-mail: long.zhang@szu.edu.cn; heyejun@126.com).

S. Gao, Q. Luo, and W. Li are with the School of Engineering and Digital Arts, University of Kent, Canterbury CT2 7NT, U.K. (e-mail: s.gao@kent.ac.uk).

Q. Li is with the School of Electronic Information and Communications, Huazhong University of Science and Technology, Wuhan 430074, China.

Color versions of one or more of the figures in this communication are available online at http://ieeexplore.ieee.org.

Digital Object Identifier 10.1109/TAP.2018.2867031

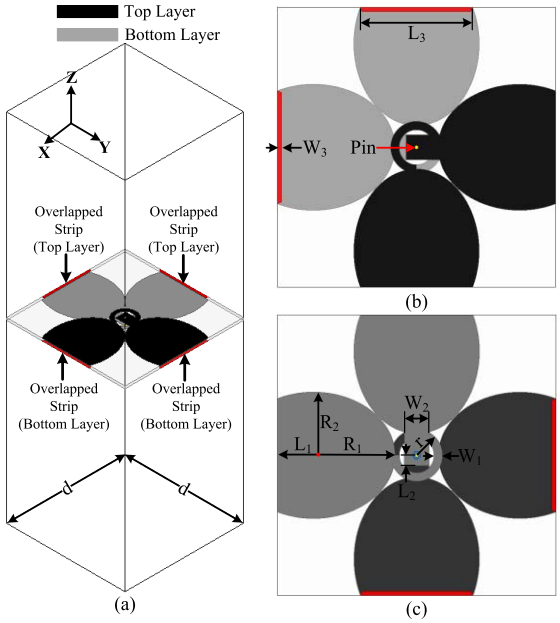

Fig. 1. Geometry of the unit cell. (a) 3-D view. (b) Top view. (c) Bottom view.

TABLE I
UNIT CELL DIMENSIONS (IN MILLIMETERS)

d	L_1	L_2	L_3	W_1	W_2	W_3	R_1	R_2	r
40	5.2	1.5	16.1	1.2	3.5	0.6	11.7	9	3.7

The proposed element is printed on both sides of a 0.813 mm-thick Rogers RO4003C substrate. As shown, two neighboring cutting-off elliptical arms are connected by a 3/4 ring-shaped phase-shift line with outer radius r and linewidth W_1. This 3/4 ring-shaped line provides 90° phase shift between the neighboring arms, which makes the crossed dipoles radiate CP wave. Besides, the top-layer arms are connected to the inner pin of a coaxial cable while the bottom-layer arms are connected to the outer conductor and no ground plane is used. To imitate an infinite TCA, the proposed element is placed in periodic boundaries with the unit cell size of $d \times d$, and four overlapped strips are utilized to provide strong capacitive coupling between adjacent elements along both the x- and y-directions. The detailed geometry dimensions of the unit cell are given in Table I.

B. Comparison With the Isolated Crossed Dipole

An isolated crossed dipole with the same size as the element used in the infinite tightly coupled crossed dipole array (TCCDA) is also simulated for a comparison. Fig. 2 shows the comparison of these two elements in terms of VSWR and AR.

As shown in Fig. 2, the simulated VSWR $<$ 3 bandwidth of the isolated element is 2–6 GHz (3:1) while the corresponding bandwidth of the tightly coupled unit cell is 0.9–6.4 GHz (7.1:1). Greatly improved impedance bandwidth at the lower frequency is observed, which is similar to those linearly polarized tightly coupled unit cell [7], [8]. Furthermore, it is shown that the AR bandwidth improves from 4–5.3 GHz (1.325:1) to 2.4–5.3 GHz (2.21:1) by the tightly coupled unit cell.

III. ANALYSIS AND DESIGN OF THE 4 × 4 CP-TCCDA

A. Analysis of the Bandwidth Enhancement

As demonstrated in Section II, the bandwidth of a CP crossed dipole can be improved by using a TCA. The enhancement of impedance bandwidth can be explained by the lengthening of the electric current or equivalently increasing of the antenna's electrical length, which decreases the array's lower limit working frequency range while the upper limit of the working frequency range is mainly controlled by the element and thus varies slightly.

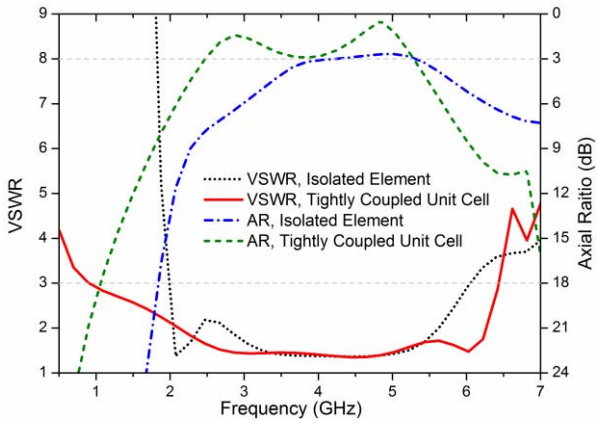

Fig. 2. Comparison of the VSWR and AR between the isolated element and the tightly coupled unit cell.

The phase difference between the two orthogonally placed dipoles is mainly controlled by the 3/4 ring-shaped phase-shift line and its length is calculated by

$$l_{\text{phase shift}} = 2\pi \times (r - W_1/2) \times 3/4 \tag{1}$$

where r, W_1, and W_2 are the parameters shown in Table I. The calculated physical length of the 3/4 ring-shaped phase-shift line is around 14.6 mm which equals a quarter of the guided wavelength at 3.08 GHz.

Considering an elliptically polarized wave $\vec{E}(z,t) = \vec{x}E_x \cos(\omega t - kz) + \vec{y}E_y \cos(\omega t - kz + \delta)$ with its AR calculated by [15]

$$\text{AR} = \frac{E_{major\ axis}}{E_{minor\ axis}} = \frac{\text{OA}}{\text{OB}}, \quad 1 \le \text{AR} \le \infty \tag{2}$$

where

$$\text{OA} = \left\{\frac{1}{2}\left[E_x^2 + E_y^2 + \left(E_x^4 + E_y^4 + 2E_x^2E_y^2\cos 2\delta\right)^{\frac{1}{2}}\right]\right\}^{\frac{1}{2}} \tag{3}$$

$$\text{OB} = \left\{\frac{1}{2}\left[E_x^2 + E_y^2 - \left(E_x^4 + E_y^4 + 2E_x^2E_y^2\cos 2\delta\right)^{\frac{1}{2}}\right]\right\}^{\frac{1}{2}}. \tag{4}$$

Since the infinite CP-TCCDA has enough electrical lengths along the x- and y-directions at 2.4 GHz, it is reasonable to deem that the magnitude of the radiated E-fields along the x- and y-directions is close to each other at 2.4 GHz, that is,

$$E_x \approx E_y. \tag{5}$$

As the phase difference introduced by the 3/4 ring-shaped phase-shift line is around 90° at 3.08 GHz, the phase difference between E_x and E_y at 2.4 GHz is

$$\delta = \frac{\pi}{2} \times \frac{2.4}{3.08} = 0.39\pi. \tag{6}$$

Substituting (5) and (6) into (2)–(4), we can calculate the AR at 2.4 GHz and yield a result of 1.425 (3.07 dB), which is very close to the simulation result shown in Fig. 2. From the above analysis and calculation result, the following conclusions are obtained.

1) The AR bandwidth enhancement of the CP-TCCDA is mainly attributed to the strong mutual coupling which enables the

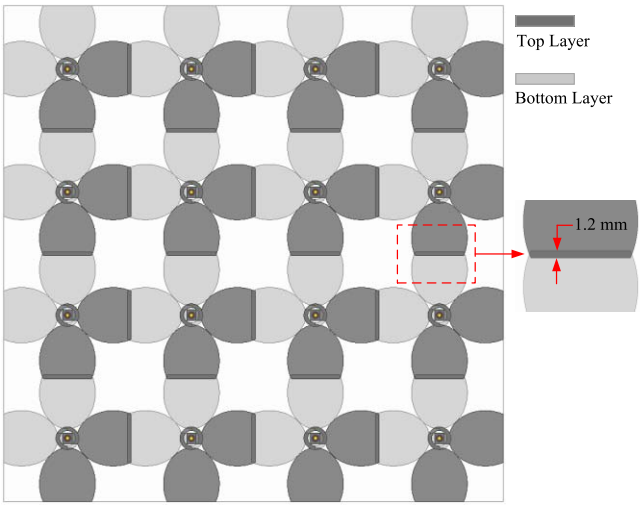

Fig. 3. Configuration of the 4 × 4 CP-TCCDA.

array to radiate more evenly along the x- and y-directions at much lower frequencies. Although the VSWR of the single isolated element at 2.4 GHz is around 2, the smaller electrical length than the CP-TCCDA may result in deterioration of the magnitude balance and possible phase difference variations between $\vec{E}_x$ and $\vec{E}_y$.

2) Although the impedance bandwidth of CP-TCCDA can reach a lower limit of 0.9 GHz, the AR bandwidth of the array cannot approach this limit. Considering that the phase difference between $\vec{E}_x$ and $\vec{E}_y$ is determined by the electrical length of the 3/4 ring-shaped phase-shift line, the phase difference between the two orthogonal E-fields at 0.9 GHz is around 26.3°. Assuming that $E_x = E_y$ and the AR at 0.9 GHz are calculated to be 12.6 dB. Notice that at this frequency, actually the magnitudes of the E-fields along the x- and y-directions may have certain differences and thus the AR should be larger than 12.6 dB. Thus, the AR bandwidth limitation of the proposed array is mainly attributed to the variation of the phase difference between the two orthogonal E-fields when the frequency changes.

B. 4 × 4 CP-TCCDA and 4 × 4 Conventional Crossed Dipole Array

To verify the above analysis and the presented concept, a 4 × 4 CP-TCCDA is designed. The configuration of the 4 × 4 CP-TCCDA is shown in Fig. 3, where the magnified photograph demonstrates the overlapped area in detail. As shown, the width of the overlapped part is 1.2 mm which is twice the width of the overlapped strip in the unit cell. The element space is 40 mm which is the same as the unit cell size given in Fig. 1. Furthermore, to make a straightforward comparison with a conventional array, a 4 × 4 conventional array using the isolated element is also designed. The element space of the 4 × 4 conventional array is chosen to be half of the free-space wavelength at 2.4 GHz (62.5 mm). With this element space, the array has much smaller coupling than the CP-TCCDA.

Fig. 4 shows the simulated E-fields of the two arrays at 2.4 GHz in a plane parallel to the array aperture at the height of 55 mm. The magnitudes of the two fields are normalized to the same scale for better comparison. As the E-fields along broadside direction relate to the array's AR bandwidth, the E-fields at the center area of each graph are of major interest. As shown, both the 4 × 4 CP-TCCDA and the 4 × 4 conventional coupled array have a rotated E-fields

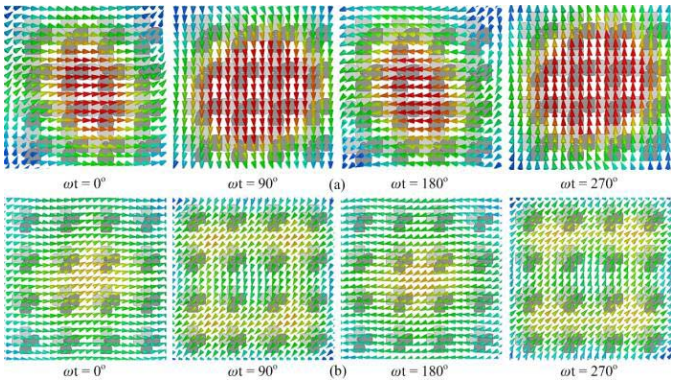

Fig. 4. Comparison of the E-fields at 2.4 GHz. (a) 4 × 4 CP-TCCDA. (b) 4 × 4 conventional array.

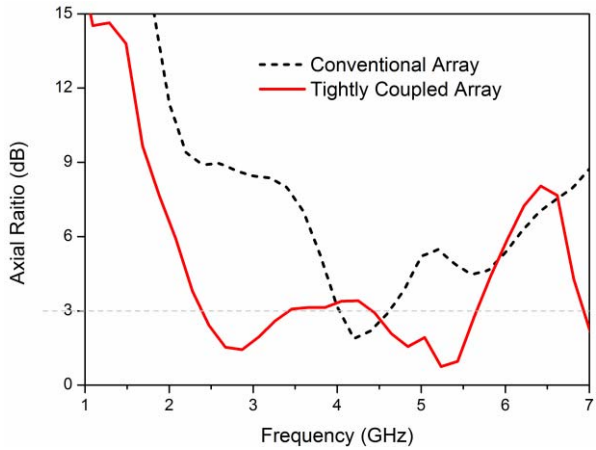

Fig. 5. Comparison of the AR between the 4 × 4 CP-TCCDA and 4 × 4 conventional crossed dipole array.

distribution at different time slots. However, the magnitudes of the E-fields of the 4 × 4 conventional coupled array are quite different for the radiated E-fields along the x- and y-directions (E_x and E_y). On the contrary, the radiated E-fields of the 4 × 4 CP-TCCDA along the x- and y-directions are nearly the same in the center area, which verifies the assumption of (5). As the phase difference between $\vec{E}_x$ and $\vec{E}_y$ of the two arrays are both determined by the 3/4 ring-shaped phase-shift line, the phase differences between $\vec{E}_x$ and $\vec{E}_y$ of the two arrays are the same at 2.4 GHz. However, the unequal (unbalanced) magnitudes of $\vec{E}_x$ and $\vec{E}_y$ of the 4 × 4 conventional coupled array result in a larger AR compared with the 4 × 4 CP-TCCDA, according to (2)–(4).

The comparison of the AR between the 4 × 4 CP-TCCDA and 4 × 4 conventional crossed dipole array is shown in Fig. 5. As shown, the 3 dB AR bandwidth of the 4 × 4 CP-TCCDA is much wider than the conventional crossed dipole array. Moreover, the simulated AR performance of the 4 × 4 CP-TCCDA is close to the simulated AR of the infinite CP-TCCDA due to the fact that the 4 × 4 CP-TCCDA is able to maintain balanced magnitudes of $\vec{E}_x$ and $\vec{E}_y$ at low frequencies.

C. 1:16 Wilkinson Power Divider Network

To feed the 4 × 4 CP-TCCDA, a 1:16 Wilkinson power divider network is designed as shown in Fig. 6. Since the CP-TCCDA achieves a 3 dB AR bandwidth from 2.4 to 5.3 GHz (2.21:1),

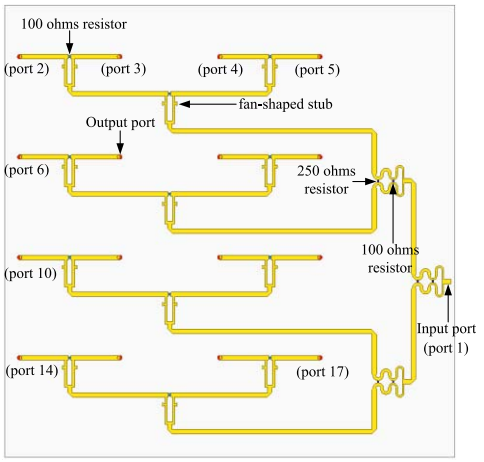

Fig. 6. 1:16 Wilkinson power divider network.

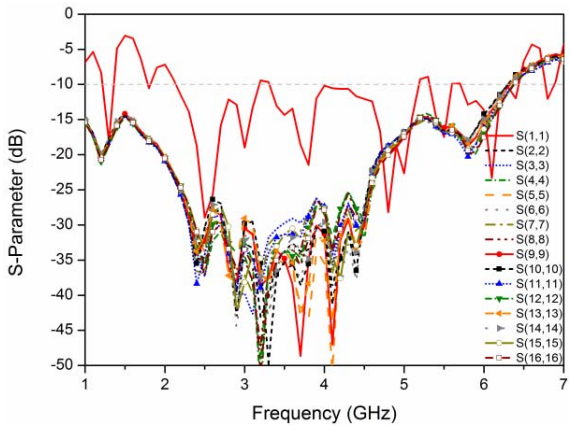

Fig. 7. Simulated reflection coefficients of the power divider network.

the bandwidth of the power divider network is designed to cover this frequency range.

The simulated reflection coefficients of all ports are shown in Fig. 7. As shown, the input port (port 1) achieves −10 dB reflection coefficient from 2.1 to 6.3 GHz while all other ports' reflection coefficients are smaller than −10 dB from 1 to 6.3 GHz. From the simulation, the input power is divided equally to the 16 output ports, and the insertion loss is around 1–2 dB from 2 to 6.3 GHz, which meets the bandwidth coverage requirement.

IV. Results and Discussion

To verify the design concept and relevant analysis, a 4 × 4 CP-TCCDA with feeding network is prototyped and measured.

A. Prototype

The fabricated 4 × 4 CP-TCCDA is shown in Fig. 8. As shown, the array is placed above an Eccosorb AN-77 absorber which helps achieve directional radiation and maintain good bandwidth performance. The thickness of the absorber is 5.7 cm while the height of the array is 12 cm. There are 16 coaxial cables with outer conductors soldered to the bottom-layer arms and inner pins soldered to the top-layer arms of the proposed array, which is demonstrated in Fig. 8 (d). These cables are then connected to the 1:16 power divider network which is shown in Fig. 9. For this array configuration,

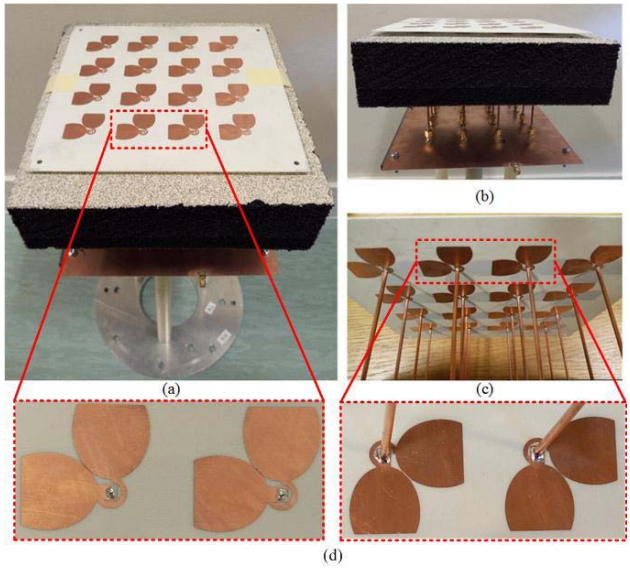

Fig. 8. 4 × 4 CP-TCCDA prototype. (a) Front view. (b) Side view. (c) Bottom view. (d) Feeding structure.

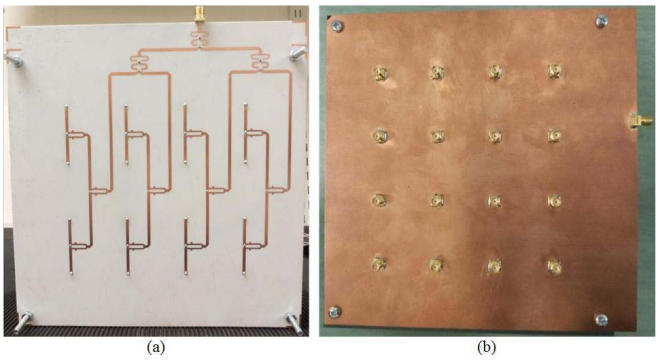

Fig. 9. 1:16 Wilkinson power divider network prototype: (a) top view and (b) bottom view (ground plane with 16 coaxial connectors).

the array height is mainly determined by the thickness of the absorber and assembling requirements.

B. VSWR and AR

The simulated and measured VSWR of the proposed 4 × 4 CP-TCCDA is shown in Fig. 10. It is worth pointing out that the simulated curve indicates the active VSWR of one center element, which is better than the VSWR of peripheral elements. As the measured result combines the VSWR of all 16 ports, the measured result is worse than the simulation result. As shown, the measured VSWR < 3 bandwidth is from 2.06 to 6.46 GHz (3.14:1). The measured VSWR is smaller than 2.5 within most of the bandwidth coverage. Compared with the simulated VSWR, ripples are constantly occurred, which is caused by the multiple reflections of the power divider network, as shown in Fig. 7.

It is noted that no obvious common-mode resonance is observed in the results. One reason may be the utilization of the absorber which helps suppress the net vertically polarized currents undergoing strong resonances. When the array is scanned, the VSWR of the array will degrade due to the unbalanced push–pull currents and the common-mode resonances [16]. Generally, the array works well when it scans to broadside and small angles but will undergo performance degradation to some extent when it scans to large angles.

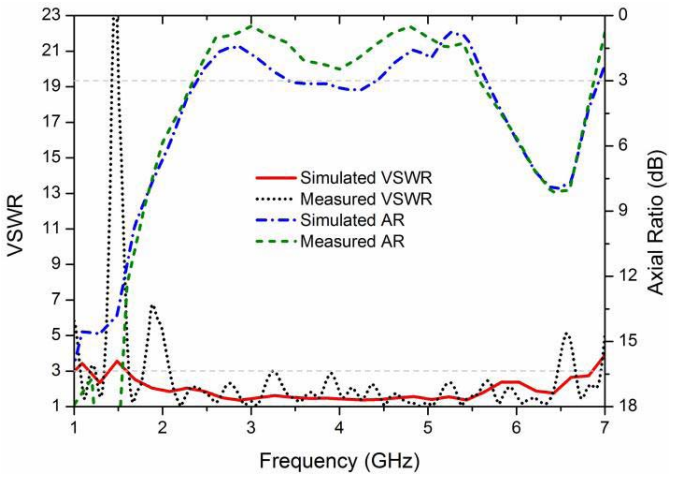

Fig. 10. Simulated and measured VSWR.

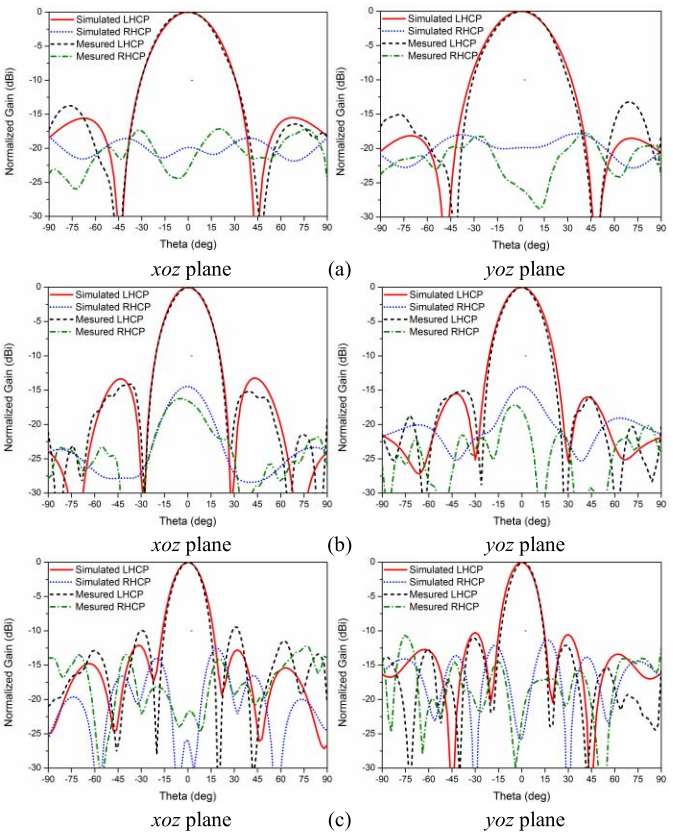

Fig. 11. Simulated and measured radiation patterns at (a) 2.6, (b) 4, and (c) 5.4 GHz.

Fig. 10 also shows the simulated and measured AR bandwidth. The measured result indicates that the proposed 4 × 4 CP-TCCDA achieves 3 dB AR bandwidth from 2.35 to 5.6 GHz (2.38:1).

C. Radiation Patterns

The simulated and measured radiation patterns are shown in Fig. 11. Good agreements between the simulation and measurement results are observed. It is also shown that the proposed array achieves undistorted beams and lower than −15 dB cross-pol over a 2.1:1 frequency range.

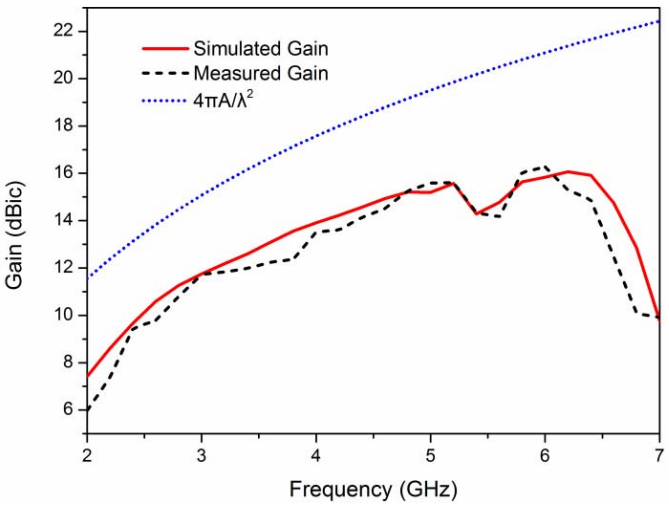

Fig. 12. Simulated and measured gain.

D. Gain

The simulated and measured gain is shown in Fig. 12. The insertion loss of the feeding network is compensated when calculating the measured gain. As shown, the antenna gain increases as frequency increases within the working bandwidth, which is similar to those reported linearly polarized TCAs. The reduction of the array gain around 5.5 GHz may be attributed to the finite size of the antenna array [17]. Moreover, an additional curve which indicates the gain of an ideal array with the same aperture size and 100% aperture efficiency is included in Fig. 12 for reference. Due to the presence of the absorber, the array gain is around 4 dB smaller than the gain of the ideal array within the operating bandwidth.

V. Conclusion

A wideband CP-TCCDA which uses the strong coupling between adjacent elements to improve the AR bandwidth of the array is proposed in this communication. Analysis is given to interpret the AR bandwidth improvement mechanism and it is found that the balanced E-fields along the x- and y-directions over a wide frequency range lead to the enhancement of AR performance. A 4×4 CP-TCCDA with feeding network is fabricated, and the measured results validate the design concept. Owing to the concurrent wide impedance bandwidth and wide AR bandwidth, the proposed CP-TCCDA is promising for applications in various wireless systems which need large bandwidth.

References

[1] J. P. Doane, K. Sertel, and J. L. Volakis, "A wideband, wide scanning tightly coupled dipole array with integrated balun (TCDA-IB)," *IEEE Trans. Antennas Propag.*, vol. 61, no. 9, pp. 4538–4548, Sep. 2013.

[2] B. A. Munk, *Finite Antenna Arrays and FSS*. Hoboken, NJ, USA: Wiley, 2003.

[3] E. Yetisir, N. Ghalichechian, and J. L. Volakis, "Ultrawideband array with 70° scanning using FSS superstrate," *IEEE Trans. Antennas Propag.*, vol. 64, no. 10, pp. 4256–4265, Oct. 2016.

[4] H. Wheeler, "Simple relations derived from a phased-array antenna made of an infinite current sheet," *IEEE Trans. Antennas Propag.*, vol. 13, no. 4, pp. 506–514, Jul. 1965.

[5] D. Cavallo and A. Neto, "A connected array of slots supporting broadband leaky waves," *IEEE Trans. Antennas Propag.*, vol. 61, no. 4, pp. 1986–1994, Apr. 2013.

[6] R. J. Bolt *et al.*, "Characterization of a dual-polarized connected-dipole array for Ku-band mobile terminals," *IEEE Trans. Antennas Propag.*, vol. 64, no. 2, pp. 591–598, Feb. 2016.

[7] J. A. Kasemodel, C.-C. Chen, and J. L. Volakis, "Wideband planar array with integrated feed and matching network for wide-angle scanning," *IEEE Trans. Antennas Propag.*, vol. 61, no. 9, pp. 4528–4537, Sep. 2013.

[8] M. H. Novak and J. L. Volakis, "Ultrawideband antennas for multiband satellite communications at UHF-Ku frequencies," *IEEE Trans. Antennas Propag.*, vol. 63, no. 4, pp. 1334–1341, Apr. 2015.

[9] S. Gao, Q. Luo, and F. Zhu, *Circularly Polarized Antennas*. Hoboken, NJ, USA: Wiley, 2013.

[10] R. Guinvarc'h and R. L. Haupt, "Connecting spirals for wideband dual polarization phased array," *IEEE Trans. Antennas Propag.*, vol. 59, no. 12, pp. 4534–4541, Dec. 2011.

[11] I. D. H. Sáenz, R. Guinvarc'h, R. L. Haupt, and K. Louertani, "A 6:1 bandwidth, low-profile, dual-polarized ring array of spiral antennas with connecting arms," *IEEE Trans. Antennas Propag.*, vol. 64, no. 2, pp. 752–756, Feb. 2016.

[12] I. Tzanidis, K. Sertel, and J. L. Volakis, "Interwoven spiral array (ISPA) with a 10:1 bandwidth on a ground plane," *IEEE Antennas Wireless Propag. Lett.*, vol. 10, pp. 115–118, 2011.

[13] J.-W. Baik, T.-H. Lee, S. Pyo, S.-M. Han, J. Jeong, and Y.-S. Kim, "Broadband circularly polarized crossed dipole with parasitic loop resonators and its arrays," *IEEE Trans. Antennas Propag.*, vol. 59, no. 1, pp. 80–88, Jan. 2011.

[14] D. K. Papantonis and J. L. Volakis, "Dual-polarized tightly coupled array with substrate loading," *IEEE Antennas Wireless Propag. Lett.*, vol. 15, pp. 325–328, 2016.

[15] C. A. Balanis, *Antenna Theory: Analysis and Design*. Hoboken, NJ, USA: Wiley, 2016.

[16] S. S. Holland and M. N. Vouvakis, "The planar ultrawideband modular antenna (PUMA) array," *IEEE Trans. Antennas Propag.*, vol. 60, no. 1, pp. 130–140, Jan. 2012.

[17] S. S. Holland, D. H. Schaubert, and M. N. Vouvakis, "A 7–21 GHz dual-polarized planar ultrawideband modular antenna (PUMA) array," *IEEE Trans. Antennas Propag.*, vol. 60, no. 10, pp. 4589–4600, Oct. 2012.